

Sustained Activation of Lyn Tyrosine Kinase In Vivo Leads to Autoimmunity

Margaret L. Hibbs,¹ Kenneth W. Harder,¹ Jane Armes,³
Nicole Kountouri,¹ Cathy Quilici,¹ Franca Casagrande,¹
Ashley R. Dunn,¹ and David M. Tarlinton²

¹Ludwig Institute for Cancer Research, Melbourne Tumour Biology Branch and ²Walter and Eliza Hall Institute of Medical Research, Royal Melbourne Hospital, Victoria 3050, Australia

³Melbourne Pathology, Royal Women's Hospital, Victoria 3053, Australia and Victorian Breast Cancer Research Consortium, Department of Pathology, University of Melbourne, Victoria 3052, Australia

Abstract

Genetic ablation of the Lyn tyrosine kinase has revealed unique inhibitory roles in B lymphocyte signaling. We now report the consequences of sustained activation of Lyn in vivo using a targeted gain-of-function mutation (Lyn^{up/up} mice). Lyn^{up/up} mice have reduced numbers of conventional B lymphocytes, down-regulated surface immunoglobulin M and costimulatory molecules, and elevated numbers of B1a B cells. Lyn^{up/up} B cells are characterized by the constitutive phosphorylation of negative regulators of B cell antigen receptor (BCR) signaling including CD22, SHP-1, and SHIP-1, and display attributes of lymphocytes rendered tolerant by constitutive engagement of the antigen receptor. However, exaggerated positive signaling is also apparent as evidenced by the constitutive phosphorylation of Syk and phospholipase C γ 2 in resting Lyn^{up/up} B cells. Similarly, Lyn^{up/up} B cells show a heightened calcium flux in response to BCR stimulation. Surprisingly, Lyn^{up/up} mice develop circulating autoreactive antibodies and lethal autoimmune glomerulonephritis, suggesting that enhanced positive signaling eventually overrides constitutive negative signaling. These studies highlight the difficulty in maintaining tolerance in the face of chronic stimulation and emphasize the pivotal role of Lyn in B cell signaling.

Key words: B cell signal transduction • Src family kinase • Lyn gain-of-function mutant mice • autoimmune disease • B cell tolerance

Introduction

The nature of the B cell response to antigen depends on the state of differentiation of the B cell, the composition, concentration, and valence of the antigen, and the cellular environment (1). In its most basic manifestation, this information is processed to allow immune responses to foreign antigens and tolerance to self. Information about antigens is gathered by molecules on the surface of immune cells and transmitted through various signaling pathways into the cell nucleus to induce a cellular response. Some signaling pathways are stimulatory and others are inhibitory and it is the integration of these signals that generates an outcome appropriate to the circumstance, be that an immune response or tolerance. An imbalance between the positive and negative signals, on the other hand, could result in an inappropriate

response leading to autoimmunity or immune deficiency. For example, mice with altered dosages of genes encoding B cell inhibitory and costimulatory receptors such as CD22, PD-1, Fc γ RIIb1, and CD19, all of which play key roles in modulating the strength of the B cell antigen receptor (BCR)* signal, are predisposed to autoimmune disease (2–8). Cytoplasmic protein tyrosine phosphatases such as SHP-1 also modulate BCR signaling (9) as exemplified by the severe B cell lymphopenia and autoantibody production of motheaten mice (10) that carry a debilitating mutation in SHP-1 (11, 12).

The Lyn tyrosine kinase is involved in both positive and inhibitory signaling pathways in B lymphocytes (13). Lyn's role in activation is mediated by the phosphorylation of

Address correspondence to Margaret L. Hibbs, Ludwig Institute for Cancer Research, Melbourne Tumour Biology Branch, P.O. Box 2008, Royal Melbourne Hospital, Victoria 3050, Australia. Phone: 61-3-9341-3155; Fax: 61-3-9341-319; E-mail: Margaret.Hibbs@ludwig.edu.au

*Abbreviations used in this paper: BCR, B cell antigen receptor; BM, bone marrow; BrdU, 5-bromo-2' deoxyuridine; [Ca²⁺]_i, intracellular calcium concentration; HEL, hen egg lysozyme; HRP, horseradish peroxidase; PLC γ 2, phospholipase C γ 2; PY, phosphotyrosine.

tyrosine residues within immunoreceptor tyrosine-based activation motifs of proteins such as Ig α , Ig β , and CD19, and the subsequent recruitment of enzymes such as Syk, phospholipase C γ 2 (PLC γ 2), and phosphatidylinositol-3 kinase (14). As a balance, there is suppression of B cell stimulation from Lyn-dependent phosphorylation of tyrosine residues within immunoreceptor tyrosine-based inhibitory motifs in proteins such as CD22, PIR-B, and Fc γ RIIb1, with the concomitant recruitment to the plasma membrane of phosphatases such as SHP-1 and SHIP-1 (15–21). Studies of Lyn-deficient mice have shown that although Lyn is functionally redundant for the positive regulation of signaling through the BCR, it is indispensable for negative regulation of signaling. Lyn-deficient B cells fail to recruit protein tyrosine phosphatases to the plasma membrane due to defects in phosphorylation of inhibitory receptors (16–19, 22). This results in defective inhibitory signaling and as a consequence, Lyn-deficient B cells are hyperresponsive to BCR stimulation and show enhanced proliferation, calcium flux, and activation of the mitogen-activated protein kinase pathway (15–19, 23). The hyperresponsive B cell phenotype almost certainly underpins the autoimmune disease that Lyn-deficient mice develop (24, 25).

The dual nature of Lyn's role in the regulation of B cell signaling makes it a potentially critical target in analyzing the development of B cell dysfunction. Having noted the effects of the absence of Lyn activity (24), we now ask what immunological consequences flow from the constitutive engagement of both stimulatory and inhibitory signaling pathways using a targeted gain-of-function Lyn tyrosine kinase mutant (Lyn^{up/up} mice). Sustained up-regulation of Lyn tyrosine kinase activity in Lyn^{up/up} mice leads to the development of B cells that have down-regulated surface IgM and costimulatory molecules, are refractory to stimulation with B cell mitogens, but show normal responses to T cell-derived signals. This phenotype is reminiscent in some respects of that defined by a model system of B cell anergy (26), although unlike this model, which uses a single self-reactive BCR chronically engaged by self-antigen, Lyn^{up/up} mice retain a full range of Ig specificities. However, in contrast to this model, Lyn^{up/up} B cells display constitutive tyrosine phosphorylation of both positive and negative regulators of BCR signaling and show exaggerated calcium fluxes in response to BCR cross-linking. Thus, their phenotype appears to be a balance between chronic negative signaling and enhanced positive signaling. Intriguingly, the mice develop circulating autoreactive antibodies, severe autoimmune glomerulonephritis, and have a significantly shorter life expectancy than wild-type mice. This eventual breakdown in tolerance might be a result of enhanced positive signaling overriding chronic negative signaling. These studies, together with those of Lyn-deficient mice, demonstrate the central role of Lyn in maintaining the equilibrium between positive and negative signaling pathways in B lymphocytes and thus in the regulation of B cell tolerance and the development of autoimmunity.

Materials and Methods

Mice. Lyn^{up/up} mice (27) were housed in microisolators and maintained as C57BL/6 \times 129/Sv intercrosses. Experiments were performed in accordance with the National Health and Medical Research Council of Australia (NH&MRC) guidelines for animal experimentation.

Primary B Cells. For Lyn expression studies, B cells were purified from Lyn^{+/+}, Lyn^{+/up}, and Lyn^{up/up} mice by FACS[®] sorting using Abs to CD45R (B220) and IgM. Pre-B cells (B220⁺ IgM⁻) and immature B cells (B220⁺ IgM⁺) were sorted from the bone marrow (BM) using appropriate gates to exclude recirculating B cells (B220^{hi} IgM⁺). B220⁺ recirculating B cells were sorted from the spleen.

To evaluate phosphorylation patterns, B cells were purified from the spleens of Lyn^{+/+}, Lyn^{up/up}, and Lyn^{-/-} mice using biotinylated B220, streptavidin MicroBeads, and MiniMACS columns (Miltenyi Biotec). B cell purity was always >85%. Purified B cells were resuspended to 10⁷ cells/ml in DME/1 mM vanadate, prewarmed for 10 min at 37°C, and stimulated with 40 μ g/ml F(ab')₂ anti-IgM or 5 μ g/ml intact rabbit anti-mouse IgM (Jackson ImmunoResearch Laboratories) to coligate BCR and Fc γ RIIb1.

Flow Cytometric Analyses. Cell preparation and FACS[®] analysis have been described (24). Cells were stained with the following monoclonal Abs: RA3-6B2 (B220), 1D3 (CD19), R6-60.2 (IgM), 7G6 (CD21), HM79b (Ig β), Cy34.1 (CD22), 1G10 (CD80), GL1 (CD86), 53.7 (CD5), 30-H12 (Thy-1.2), goat anti-mouse IgD, 187.1 (Ig κ), JC5 (Ig λ), S7 (CD43), B3B4 (CD23), M1/69 (HSA), and M5/114 (Ia^{b,d}).

Proliferation Assays. B cells, purified by FACS[®] sorting, were cultured at a density of 5 \times 10⁵ per ml in complete RPMI and stimulated as previously described (24).

Colony Assays. B cell progenitors were determined in 1 ml semisolid 0.3% agar cultures (28). Colony formation was stimulated by the combination of 200 ng/ml interleukin-7 (R&D Systems), 300 ng/ml Flt3 ligand, and 50 ng/ml stem cell factor (provided by N. Nicola, Walter and Eliza Hall Institute of Medical Research, Melbourne, Australia). Plates were incubated at 37°C in 7% CO₂ in air and colonies were enumerated on day 5.

B Cell Life Span Studies. 5-bromo-2' deoxyuridine (BrdU; Sigma-Aldrich) was administered in drinking water (0.50 mg/ml BrdU, 1% glucose) to 8-wk-old Lyn^{+/+} and Lyn^{up/up} mice for 7 d. Single cell suspensions of spleen were depleted of RBCs and stained for surface CD19 and nuclear BrdU (29). The data are presented as the percentage of splenic CD19⁺ B cells that are BrdU⁺.

Intracellular Calcium Concentration ([Ca²⁺]_i) Measurement. Spleen cells were loaded with 2 μ M Indo-1 (Molecular Probes Inc.) for 40 min at 37°C, stained with anti-B220, and resuspended at 10⁷ cells/ml. Baseline fluorescence was established using an LSR (Becton Dickinson) and BCR ligation initiated by the addition of F(ab')₂ goat anti-IgM to a final concentration of 40 μ g/ml. The subsequent calcium flux was followed in B220⁺ B cells (16).

ELISA and Immunizations. Total serum Ig titers were determined by ELISA using goat anti-mouse Ig as a capture reagent and developed either with biotinylated isotype-specific goat sera and streptavidin-conjugated horseradish peroxidase (HRP), or Abs directly conjugated with HRP (Southern Biotechnology Associates, Inc.). Purified myeloma proteins (Sigma-Aldrich) were used as standards. NP-KLH (100 μ g in alum) and DNP-dextran (10 μ g in PBS; reference 30), were administered by intraperitoneal injection. Serum titers of antigen-specific Ig were determined using an NP-specific ELISA (31).

Immunohistochemistry. Splens were embedded in OCT compound and snap frozen in a bath of isopentane in liquid nitrogen. 5- μ M cryostat sections were fixed in acetone and air-dried before staining. Sections were rehydrated in PBS and endogenous peroxidase activity was blocked by incubation with 0.3% H_2O_2 . Sections stained to reveal B and T cells were first incubated with rat anti-mouse B220 followed by HRP-conjugated mouse anti-rat kappa (BD Biosciences). Sections were blocked with normal rat serum and then stained with biotinylated rat anti-mouse CD3 (KT3) followed by streptavidin-conjugated alkaline phosphatase (Southern Biotechnology Associates, Inc.). HRP was detected with the AEC Substrate Kit for Peroxidase (Vector Laboratories) and streptavidin with the VECTOR Blue Alkaline Phosphatase Substrate Kit III (Vector Laboratories) in the presence of 2 mM levanisole. Sections stained to reveal marginal zone B cells were first incubated with HRP-conjugated goat anti-mouse IgM (Southern Biotechnology Associates, Inc.) and biotinylated rat anti-mouse IgD (clone 11-26C) followed by streptavidin-conjugated alkaline phosphatase (Southern Biotechnology Associates, Inc.). Color development was performed as it had been for B and T cell staining.

Histology and Immunofluorescence. Histology was performed exactly as previously described (24). Antinuclear Abs were detected using sera at 1:100 (24). Kidneys were frozen in OCT embedding compound and immune complexes were detected with either fluoresceinated sheep anti-mouse Ig or fluoresceinated goat anti-mouse IgG (Silenus Laboratories).

Cell Lysis, Immunoprecipitation, Western Blotting, and Kinase Assays. Cells were lysed for 30 min at 5×10^7 /ml in buffer containing 1% NP-40, 100 mM NaCl, 10 mM Tris-HCl, pH 7.5, 2 mM EDTA, 1 mM pepabloc, 1 mM aprotinin, and 1 mM sodium orthovanadate, and nuclei were removed by centrifugation at 13,000 rpm. Protein concentrations of individual samples were estimated using the BCA protein estimation kit (Pierce Chemical Co.). Abs used for immunoprecipitation and Western blotting included the following: rabbit anti-Lyn (Santa Cruz Biotechnology, Inc.), mouse anti-phosphotyrosine (PY; 4G10; Upstate Biotechnology), rabbit anti-SHP-1 (provided by H.-C. Cheng, University of Melbourne, Melbourne, Australia), rat anti-CD22 (Cy34.1; BD Biosciences), rabbit anti-CD22 (provided by P. Crocker, Dundee University, Dundee, United Kingdom), rabbit anti-SHIP-1 (BD Biosciences), rabbit anti-PLC γ 2 (Q-20; Santa Cruz Biotechnology, Inc.), and rabbit anti-Syk (provided by J. Bolen, DNAX Research Institute of Molecular and Cellular Biology, Palo Alto, CA). Blots were developed with HRP-conjugated goat anti-rabbit, sheep anti-mouse antiserum, or protein A, and the enhanced chemiluminescent system (Amersham Biosciences). Autokinase reactions were performed as previously described (24) using equalized amounts of Lyn protein as determined by densitometry of Western blots.

Results

Altered Lyn Protein Levels and Signaling in *Lyn^{up/up}* B Cells. To understand further how Lyn regulates signaling thresholds, we have characterized B cells in mice expressing a constitutively activated form of Lyn. These mice, designated *Lyn^{up/up}*, carry a single point mutation (Y508F) in the *Lyn* gene in a sequence that negatively regulates Lyn activity (27). Our previous biochemical studies on macrophages from *Lyn^{up/up}* mice have demonstrated that total cellular levels of Lyn protein are regulated by the activation state of the enzyme. *Lyn^{Y508F}* protein is unstable and subject to

ubiquitination-dependent degradation (27). Consequently, Lyn protein levels are reduced in *Lyn^{up/up}* B cells and to a lesser extent in *Lyn^{+/up}* B cells (Fig. 1 a). However, al-

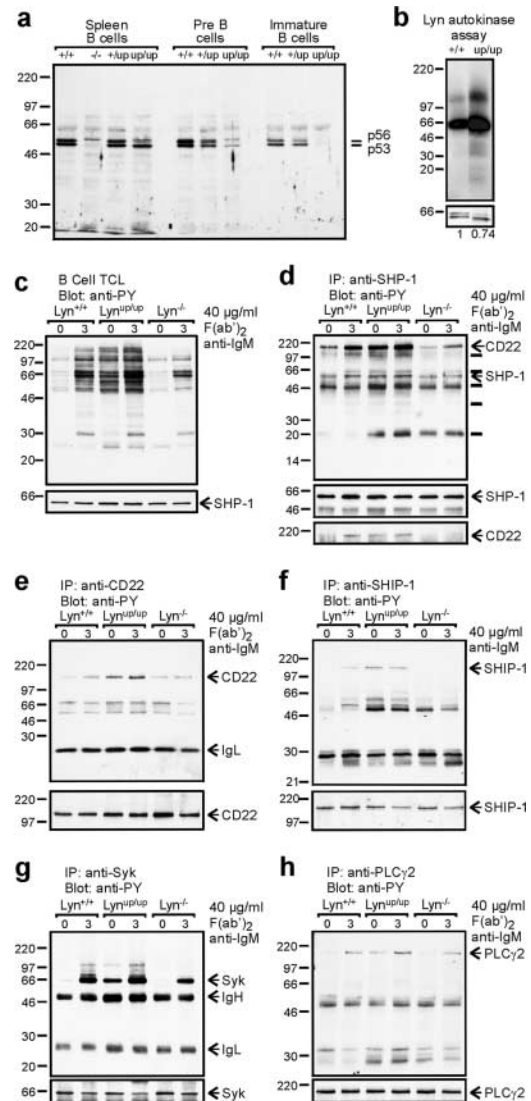


Figure 1. Altered Lyn protein levels and signaling in primary B cells from Lyn mutant mice. (a) Mature B cells were purified from the spleen (Spleen B cells) and Pre-B and immature B cells were purified from the BM of the indicated mice (+/+, *Lyn^{+/+}*; -/-, *Lyn^{-/-}*; +/up, *Lyn^{+/up}*; up/up, *Lyn^{up/up}*) by FACS[®] sorting. Total cell lysates (TCL; 5×10^6 cell equivalents for mature and Pre-B cells and 2.5×10^6 cell equivalents for immature B cells) were immunoblotted with anti-Lyn Abs. The p56 and p53 isoforms of Lyn are indicated. (b) Lyn kinase activity. Equalized levels of Lyn protein (bottom, including densitometric measurements) immunoprecipitated from *Lyn^{+/+}* (+/+) and *Lyn^{up/up}* (up/up) B cells were subjected to autokinase reactions. (c) Primary B cells from *Lyn^{+/+}*, *Lyn^{up/up}*, and *Lyn^{-/-}* mice were stimulated for 0 or 3 min with 40 μ g/ml F(ab')₂ anti-IgM. 25 μ g TCLs were immunoblotted with anti-PY. The blot was stripped and reprobed with anti-SHP-1 as a protein loading control. (d) SHP-1 was immunoprecipitated from the indicated B cell lysates and immunoblotted with anti-PY. The blot was stripped and reprobed with anti-SHP-1 (middle) and an antiserum to CD22 (bottom) to demonstrate coassociation of SHP-1 and phospho-CD22. CD22 (e), SHIP-1 (f), Syk (g), and PLC γ 2 (h) were immunoprecipitated from the indicated B cell lysates and immunoblotted with anti-PY. Blots were stripped and reprobed with the indicated antibodies to ensure equal protein loading.

though Lyn^{up} protein is diminished at all stages of B cell development that were examined, the enzymatic activity of Lyn^{Y508F} is enhanced two- to threefold (Fig. 1 b).

Unstimulated splenic Lyn^{up/up} B cells exhibit enhanced tyrosine phosphorylation of specific proteins compared with either Lyn^{+/+} or Lyn^{-/-} B cells (Fig. 1 c). After BCR cross-linking, Lyn^{+/+} B cells show dramatically enhanced numbers of tyrosine phosphorylated proteins, whereas Lyn^{up/up} B cells show only a modest increase in already elevated levels (Fig. 1 c). The increase in tyrosine phosphorylation in Lyn^{up/up} B cells after BCR stimulation might be due to either the mobilization of Lyn into the BCR complex or the recruitment and activation of other kinases such as Fyn, Blk, and Syk. Lyn^{-/-} B cells show diminished antigen-induced tyrosine phosphorylation compared with Lyn^{+/+} B cells (23, 25). These results suggest that Lyn^{up/up} B cells exist in vivo in a state of chronic stimulation.

The impact of the Lyn gain-of-function mutation on B cell signaling was determined by measuring the phosphorylation status of key regulatory molecules (Fig. 1, d-h). We first analyzed negative regulatory phosphatases and immune inhibitory receptors known to be phosphorylated in a Lyn-dependent fashion (16-19). Tyrosine phosphorylated SHP-1 was detectable in unstimulated Lyn^{+/+} B cells and at clearly increased levels in unstimulated Lyn^{up/up} B cells (Fig. 1 d). Several tyrosine-phosphorylated proteins coprecipitated with phospho-SHP-1 in unstimulated Lyn^{up/up} B cells and to a proportionately lesser degree in unstimulated Lyn^{+/+} and Lyn^{-/-} B cells (Fig. 1 d). The phosphorylation of these proteins appears to be regulated by Lyn, with previous studies suggesting they include CD22, PIR-B, p62dok, and BLNK (16-21, 32, 33). One coprecipitating protein was identified as CD22 by reprobing the blot with a CD22-specific antiserum (Fig. 1 d, bottom). Direct immunoprecipitation of CD22 shows that CD22 is hypertyrosine phosphorylated in unstimulated Lyn^{up/up} B cells (Fig. 1 e). Although the phosphorylation status of CD22 increases after BCR stimulation of Lyn^{+/+} and Lyn^{up/up} B cells, no such increase is seen in Lyn^{-/-} B cells (Fig. 1 e), consistent with previous reports (16-19). Coligation of FcγRIIb1 with the BCR leads to the inhibition of BCR-mediated signaling largely via recruitment of the SH2-containing inositol phosphatase SHIP-1 to the immunoreceptor tyrosine-based inhibitory motifs of FcγRIIb1 (34, 35). SHIP-1 is hypertyrosine phosphorylated in unstimulated Lyn^{up/up} B cells, but only visibly phosphorylated in Lyn^{+/+} B cells after BCR stimulation (Fig. 1 f). In sharp contrast, SHIP-1 is hypotyrosine phosphorylated in B cells from Lyn^{-/-} mice, regardless of their stimulation status (Fig. 1 f). In keeping with the close functional association between SHIP-1 activation and FcγRIIb1 phosphorylation, the phosphorylation status of FcγRIIb1 in Lyn^{+/+}, Lyn^{up/up}, and Lyn^{-/-} B cells mirrored that of SHIP-1 (not depicted).

Next, we examined the consequences of constitutive Lyn activation on positive signaling pathways emanating from the BCR. Syk kinase promotes B cell activation by recruiting downstream targets such as PLCγ2, the activation of which results in intracellular calcium flux (36).

Minimal tyrosine-phosphorylated Syk was observed in unstimulated Lyn^{+/+} B cells but the level increased dramatically after BCR cross-linking. In contrast, phospho-Syk was clearly detectable in unstimulated Lyn^{up/up} B cells, and this was enhanced by BCR cross-linking (Fig. 1 g). As previously reported (23), the increase in Syk phosphorylation after BCR cross-linking of Lyn^{-/-} B cells is less dramatic than in controls (Fig. 1 g). Like Syk, tyrosine-phosphorylated PLCγ2 was present in unstimulated Lyn^{up/up} B cells and its level was increased by BCR ligation (Fig. 1 h). In contrast, phospho-PLCγ2 was only detectable in Lyn^{+/+} or Lyn^{-/-} B cells after BCR stimulation (Fig. 1 h). Collectively, these results demonstrate that both negative and positive signal transduction pathways in Lyn^{up/up} B cells are constitutively activated.

Characteristics of Lyn^{up/up} Mice. To determine the effect of the Lyn gain-of-function mutation on the B cell compartment, we performed analyses of primary and secondary lymphoid tissue of 8-wk-old Lyn^{+/+}, Lyn^{+/up}, and Lyn^{up/up} mice (Figs. 2-4). Spleen cellularity was reduced in both Lyn^{+/up} and Lyn^{up/up} mice whereas white blood cell counts

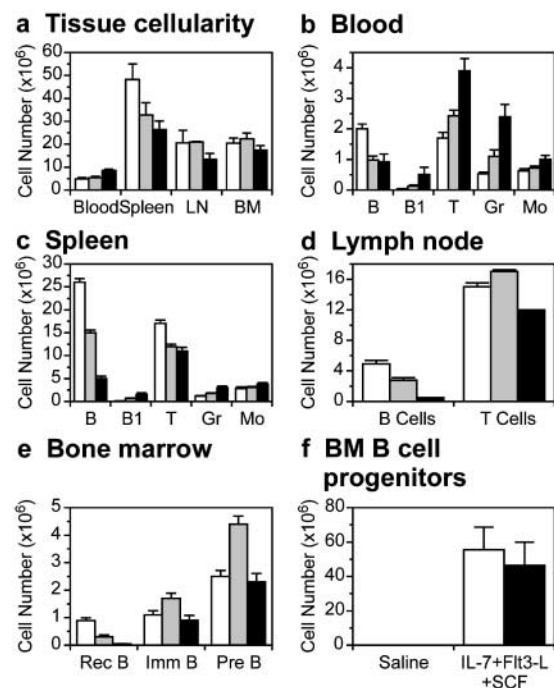


Figure 2. Cellularity and composition of lymphoid tissue in 8-wk-old Lyn^{+/+}, Lyn^{+/up}, and Lyn^{up/up} mice. (a) Nucleated cells in lymphoid tissue in Lyn^{+/+}, Lyn^{+/up}, and Lyn^{up/up} mice. Numbers represent per ml blood, per whole spleen, per mesenteric lymph nodes, and per femur. (b) Numbers of conventional B cells, B1 cells, T cells, granulocytes (Gr), and monocytes (Mo) in blood and (c) spleen of Lyn^{+/+}, Lyn^{+/up}, and Lyn^{up/up} mice. (d) Numbers of B and T cells in mesenteric lymph nodes of Lyn^{+/+}, Lyn^{+/up}, and Lyn^{up/up} mice. (e) Numbers of recirculating B cells (Rec B), immature B cells (Imm B), and Pre-B cells in the BM of Lyn^{+/+}, Lyn^{+/up}, and Lyn^{up/up} mice. Data in a-e is compiled from nine mice in three experiments, except B cell and B1 cell numbers in blood and spleen, which were compiled from six mice in two experiments. Data is mean \pm standard error. (f) BM B cell progenitors in Lyn^{+/+} and Lyn^{up/up} mice. Numbers are the mean \pm standard deviation for five mice of each genotype. For a-f, white bars, Lyn^{+/+}; gray bars, Lyn^{+/up}; black bars, Lyn^{up/up}.

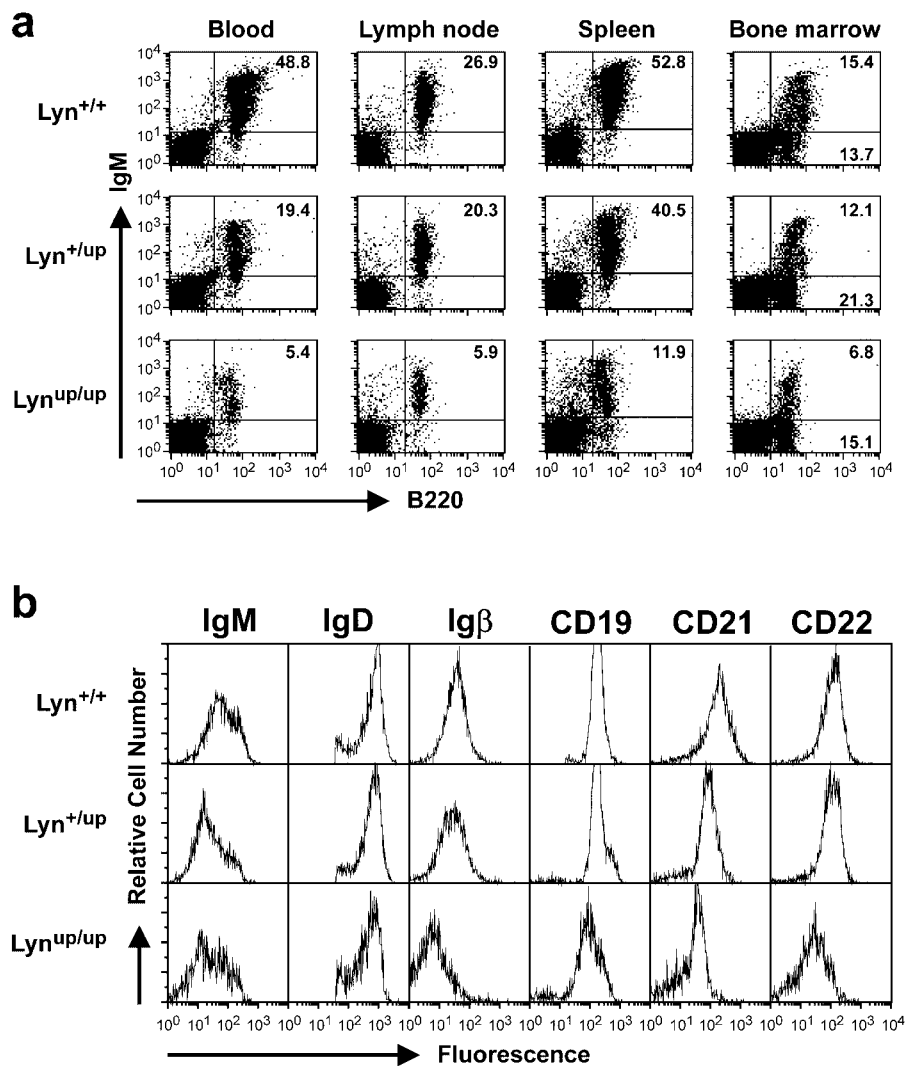


Figure 3. Lyn^{up/up} mice have reduced levels of recirculating B cells. (a) Representative two-color fluorescence analysis of lymphoid tissues from 8-wk-old Lyn^{+/+}, Lyn^{+up}, and Lyn^{up/up} mice. Staining was performed with Abs against B220 and IgM to determine proportions of B cells and levels of surface IgM. The mean fluorescence intensity of IgM on peripheral blood B cells from Lyn^{+/+}, Lyn^{+up}, and Lyn^{up/up} mice is 163, 101, and 103, respectively, on lymph node B cells is 300, 163, and 213, respectively, and on splenic B cells is 196, 122, and 133, respectively. (b) Representative single-color FACS[®] analysis of splenic B220⁺ cells from 8-wk-old Lyn^{+/+}, Lyn^{+up}, and Lyn^{up/up} mice. Staining was performed with Abs against the indicated cell surface molecules to assess expression level.

were elevated in Lyn^{up/up} mice (Fig. 2 a), presumably due to an increase in neutrophils (27). Lyn^{up/up} mice showed an overall reduction in B cells: twofold in peripheral blood, fivefold in spleen, 10-fold in lymph node, and 20-fold in the recirculating B cell compartment of the BM (Fig. 2, b–e, and Fig. 3 a). The B cell deficiency in heterozygous Lyn^{+up} mice was less severe than in homozygous mice, being approximately twofold in all lymphoid tissues. Numbers of pro-B, pre-B, and immature B cells in the BM of Lyn^{up/up} mice were not significantly different from controls (Fig. 2 e and Fig. 3 a) and B cell colony assays demonstrated no significant change in the numbers of B cell progenitors (Fig. 2 f). Although the BM results suggest that B cell development is not blocked in Lyn^{up/up} mice, levels of IgM on the surface of immature Lyn^{up/up} B cells are reduced by ~35% (not depicted). Peripheral B cells from Lyn^{up/up} and Lyn^{+up} mice also express lower surface IgM (Fig. 3, a and b), Igβ, CD19, CD21, and CD22 (Fig. 3 b), whereas IgD (Fig. 3 b) and MHC class II (not depicted) are unaffected.

Peripheral blood and spleen from Lyn^{up/up} and Lyn^{+up} mice had a variable increase in a population of cells that

were IgM⁺ B220^{lo} (Fig. 4). Additional analyses of this population revealed the expression of CD19 and CD5 (Fig. 4). Accordingly, these cells have been designated B1a B lymphocytes. Despite significant variation in the frequency of B1a B cells between Lyn^{up/up} mice, on average we found this population to be elevated approximately twofold in the spleen and 10-fold in peripheral blood (Fig. 2, b and c). B1a B cells were elevated in the peripheral blood of Lyn^{+up} mice but to a lesser degree than Lyn^{up/up} mice. Lyn^{up/up} mice show a twofold increase in cellularity in the peritoneum (not depicted), which is due to elevated numbers of CD19⁺ CD5⁺ B220^{lo} B1a cells (Fig. 4). B1b (CD5⁻ B220^{lo}) and T cell populations appeared unaffected, whereas conventional B cells were dramatically reduced in Lyn^{up/up} peritoneum, in keeping with their diminution in other lymphoid tissues (Fig. 4).

B Cell Function in Lyn^{up/up} Mice. The reduced population of mature B cells in the periphery of Lyn^{up/up} mice prompted us to investigate their functional capacity. B220^{hi} B cells were purified by FACS[®] sorting from Lyn^{up/up} spleen, thereby excluding B1 cells. Although Lyn^{+/+} B

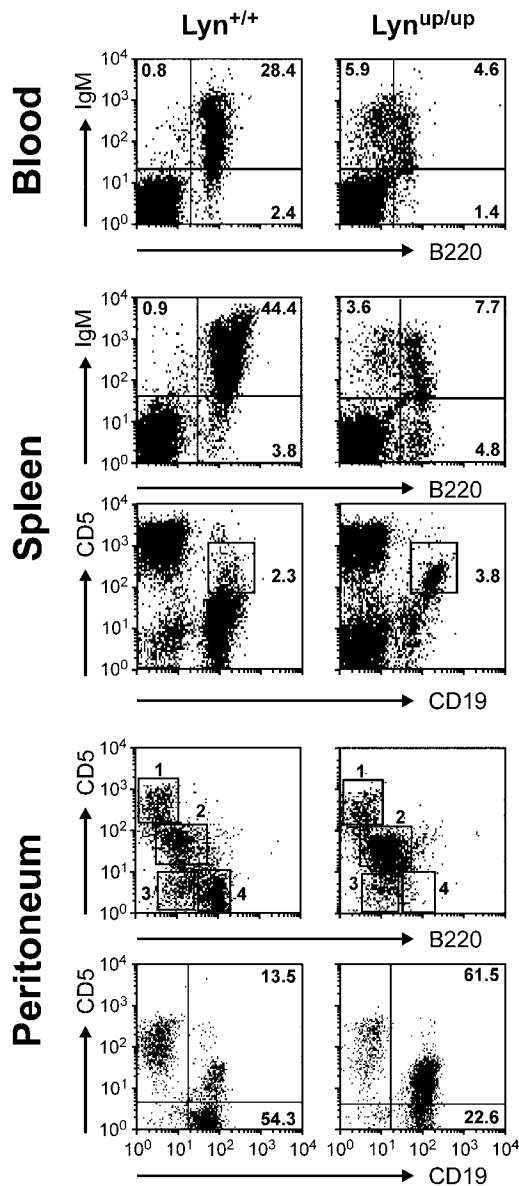


Figure 4. $Lyn^{up/up}$ mice have increased numbers of B1 cells. Two-color fluorescence analysis of blood, spleen, and peritoneal lymphoid cells from 8-wk-old $Lyn^{+/+}$ and $Lyn^{up/up}$ mice. Blood and spleen cells were stained with B220 and IgM to identify $IgM^+ B220^lo$ B1 cells. Spleen cells were also stained with CD19 and CD5 Abs to show $CD19^{hi} CD5^+$ B1a cells in $Lyn^{up/up}$ spleen (boxed region). Peritoneal cells were stained using Abs to B220 and CD5 to identify: Region 1, T cells ($Lyn^{+/+}$, 14.4%; $Lyn^{up/up}$, 13.0%), Region 2, B1a B cells ($Lyn^{+/+}$, 34.6%; $Lyn^{up/up}$, 76.1%), Region 3, B1b B cells ($Lyn^{+/+}$, 9.4%; $Lyn^{up/up}$, 4.3%), and Region 4, B2 cells ($Lyn^{+/+}$, 31.7%; $Lyn^{up/up}$, 1.8%). Alternatively, peritoneal B1a cells were revealed with Abs to CD19 and CD5.

cells proliferated well in response to 1 μ g/ml anti-IgM, $Lyn^{up/up}$ B cells were nonresponsive (Fig. 5 a). At 10 μ g/ml anti-IgM, $Lyn^{up/up}$ B cells gave a response that was seven-fold lower than that of $Lyn^{+/+}$ B cells (Fig. 5, a and b). $Lyn^{up/up}$ B cells were also poorly responsive to LPS (Fig. 5 b), but could respond normally to CD40 ligand plus interleukin-4 stimulation (Fig. 5, a and b). These results highlight the differences between $Lyn^{up/up}$ and $Lyn^{-/-}$ B cells,

which exhibit heightened responses to anti-IgM stimulation (15, 23).

B Cell Turnover in $Lyn^{up/up}$ Mice. The decreased numbers of peripheral B cells in $Lyn^{up/up}$ mice suggested an increased rate of B cell turnover. To measure this, we examined the incorporation of BrdU-labeled B cells into the splenic compartment. After 7-d labeling, 28% of $CD19^+$ B cells in the spleens of $Lyn^{+/+}$ mice had been replaced by BrdU $^+$ B cells compared with nearly 60% in $Lyn^{up/up}$ spleens (Fig. 5 c). These results reveal a far greater proportion of short-lived B cells in $Lyn^{up/up}$ mice, suggesting defects in either B cell survival or maturation.

Calcium Signaling in $Lyn^{up/up}$ B Cells. Although $Lyn^{up/up}$ B cells showed dramatic diminution of in vitro proliferative responses and constitutive activation of inhibitory signaling pathways, the enhanced tyrosine phosphorylation of Syk and PLC γ 2 in resting $Lyn^{up/up}$ B cells suggested that some positive signaling pathways remained functional. Therefore, we investigated calcium responses in B cells from $Lyn^{+/+}$ and $Lyn^{up/up}$ mice. Upon BCR cross-linking, B cells from both strains of mice showed a prompt rise in $[Ca^{2+}]_i$ followed by a gradual decline (Fig. 5 d). The maximum amplitude reached after cross-linking IgM was consistently higher in $Lyn^{up/up}$ B cells (Fig. 5 d), possibly reflecting the hyperactivation of PLC γ 2 (Fig. 1 h). Although no significant differences in the kinetics of decline was found, variable elevation in basal $[Ca^{2+}]_i$ was observed (Fig. 5 d). Thus, the calcium response of $Lyn^{up/up}$ B cells shows that BCR cross-linking dependent positive signaling pathways are enhanced despite the presence of constitutively active Lyn and engagement of inhibitory enzymes and receptors.

Immunoglobulin Levels in $Lyn^{up/up}$ Mice. To determine if the low number of peripheral B cells in $Lyn^{up/up}$ and $Lyn^{+/up}$ mice and their impaired in vitro responses had functional corollaries, serum immunoglobulin levels in $Lyn^{up/up}$ and $Lyn^{+/up}$ mice were investigated. Surprisingly, $Lyn^{up/up}$ mice had two- to threefold elevated levels of serum IgM (Fig. 6 a), possibly reflecting their increased numbers of B1a B cells. However, although B1 B cells also secrete IgA and IgG3 (37), $Lyn^{+/up}$ and $Lyn^{up/up}$ mice had normal serum IgA levels and 10-fold reduced serum IgG3 (Fig. 6 a). $Lyn^{up/up}$ mice also had 10-fold lower levels of serum IgG1 compared with control mice, whereas levels of serum IgG2b were unchanged (Fig. 6 a). Serum IgE levels were reduced by 10-fold in both $Lyn^{+/up}$ and $Lyn^{up/up}$ mice compared with control mice (Fig. 6 a). This contrasts with Lyn-deficient mice, which have 10-fold higher IgE levels than control mice and heightened sensitivity to interleukin-4 signaling (38).

Immune Responses in $Lyn^{up/up}$ Mice. Next, we examined the consequences of the $Lyn^{up/up}$ mutation on the B cell response to antigen. $Lyn^{+/+}$, $Lyn^{+/up}$, and $Lyn^{up/up}$ mice were challenged with the T cell-independent antigen DNP-dextran, and levels of anti-TNP Ab (cross-reactive with DNP) in serum were measured at regular times after immunization. Both $Lyn^{+/up}$ and $Lyn^{up/up}$ mice had reduced levels of anti-TNP Ab 5 d after immunization compared

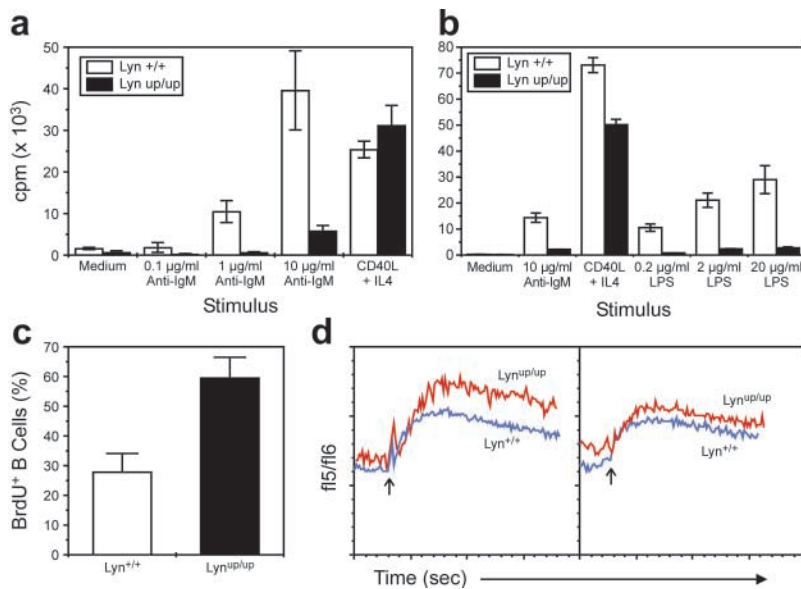
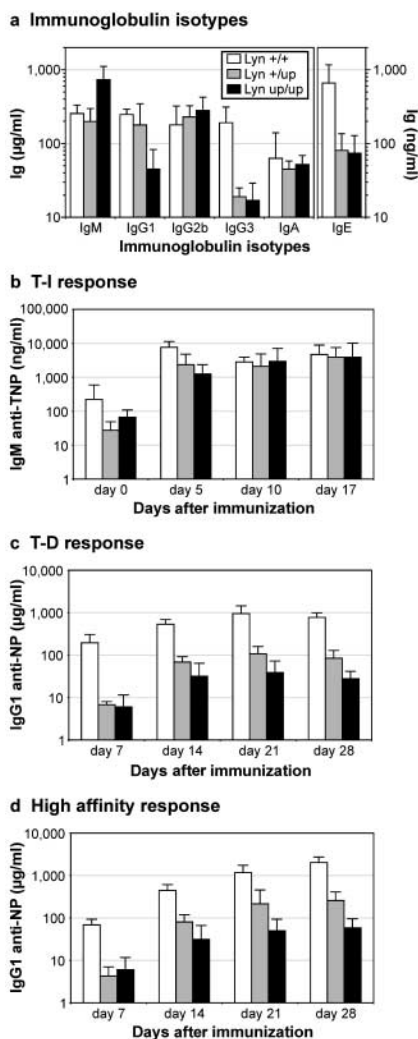


Figure 5. Proliferation, turnover, and calcium responses of $Lyn^{+/+}$ and $Lyn^{up/up}$ B lymphocytes. 5×10^4 FACS[®]-sorted splenic B cells from $Lyn^{+/+}$ mice (open bars) and $Lyn^{up/up}$ mice (solid bars) were cultured in the presence of (a) the indicated concentrations of anti-IgM or CD40 ligand plus interleukin-4 for 2 d, and in (b) the indicated concentrations of LPS, 10 μ g/ml anti-IgM, or CD40 ligand plus interleukin-4 for 3 d. (c) Turnover of peripheral B lymphocytes by incorporation of BrdU. Spleen cells from BrdU-treated $Lyn^{+/+}$ mice (open bars) and $Lyn^{up/up}$ mice (solid bars) were stained for surface CD19 and intranuclear BrdU to determine the percentage of BrdU⁺ B cells. Data is representative of two experiments in which five mice of each genotype were analyzed. (d) Changes in $[Ca^{2+}]_i$ induced by cross-linking surface IgM on Indo-1-loaded spleen cells from $Lyn^{+/+}$ and $Lyn^{up/up}$ mice. The fluorescence ratio of the cells (f15/f16) was measured by flow cytometry and B cells were identified by counter-staining with anti-B220. Cross-linking reagent was added at 60 s (arrow) and the measurement continued for 300 s. Two representative examples from three experiments involving six mice of each genotype are shown with the response of $Lyn^{+/+}$ B cells depicted in blue and $Lyn^{up/up}$ B cells in red.



with $Lyn^{+/+}$ mice, but by 10 and 17 d after immunization, levels of anti-TNP Ab were normal (Fig. 6 b). This unexpected response to a T cell-independent antigen might be a reflection of the larger B1 B cell population in $Lyn^{+/up}$ and $Lyn^{up/up}$ mice, because B1 B cells have been reported to respond to α 1-3 dextran (39).

T cell-dependent immune responses in $Lyn^{+/+}$, $Lyn^{+/up}$, and $Lyn^{up/up}$ mice were examined after immunization with NP-KLH. Compared with $Lyn^{+/+}$ animals, both $Lyn^{+/up}$ and $Lyn^{up/up}$ mice had significantly lower titers of NP-specific IgG1 7 d after immunization (Fig. 6 c). The titers of NP-specific Ab in all groups of mice increased during the next 2 wk and were maximal 3 wk after immunization, although the titers in $Lyn^{+/up}$ and $Lyn^{up/up}$ mice were only 10 and 5% of control levels, respectively. The proportion of high affinity anti-NP Ab was the same in all groups (Fig. 6 d). In addition, all mice responded to secondary challenge, although the level of Ab in $Lyn^{+/up}$ and $Lyn^{up/up}$ mice never reached that made by $Lyn^{+/+}$ mice (not depicted). The reduced levels of NP-specific Ab in $Lyn^{+/up}$ and $Lyn^{up/up}$ mice may reflect either their reduced numbers of mature B cells or the consequences of constitutive activation of negative regulatory pathways in the responding B cells.

Spleen and Lymph Node Histology in $Lyn^{up/up}$ Mice. To determine if spleen or lymph node architecture was dis-

Figure 6. Immunoglobulin levels and immune responses. (a) Levels of immunoglobulin isotypes in the serum of 8–20 unchallenged $Lyn^{+/+}$, $Lyn^{+/up}$, and $Lyn^{up/up}$ mice. (b) Specific IgM response of a group of six $Lyn^{+/+}$, $Lyn^{+/up}$, and $Lyn^{up/up}$ mice at the indicated times after immunization with 10 μ g DNP-dextran. Data is representative of two experiments. (c) Specific IgG1 response of a group of six $Lyn^{+/+}$, $Lyn^{+/up}$, and $Lyn^{up/up}$ mice at the indicated times after immunization with 100 μ g NP-KLH. Data is representative of two experiments. (d) High affinity IgG1 response of the group of mice indicated in c. Data is representative of two experiments. Data are mean \pm standard deviation. For a–d, white bars, $Lyn^{+/+}$; gray bars, $Lyn^{+/up}$; black bars, $Lyn^{up/up}$.

rupted in $Lyn^{up/up}$ mice, histological sections were examined. Like $Lyn^{+/+}$ spleen, $Lyn^{up/up}$ spleen contained lymphoid follicles, although germinal centers were not apparent and there was a loss of red/white pulp definition (Fig. 7, a–d). Surprisingly, large numbers of multinucleate giant cells were present within lymphoid follicles and in follicle marginal zones (Fig. 7, b and d). Multinucleate giant cells were also found in lymph nodes, liver, and within the thymus where they were concentrated around the medulla/cortex interface (not depicted). SIRP α , a protein that is tyrosine phosphorylated in a Lyn -dependent manner (27), is reported to be involved in macrophage fusion (40), suggesting that this phenotype may arise through its dysregulated activity in $Lyn^{up/up}$ macrophages.

To determine whether splenic white pulp was disorganized in $Lyn^{up/up}$ mice, sections were analyzed by immuno-

histochemistry (Fig. 7, e–j). B220 and CD3 staining confirmed the substantial deficit of B cells in $Lyn^{up/up}$ spleen and moderate reduction in $Lyn^{+/up}$ spleen. Formation of the B cell follicle is abnormal in $Lyn^{up/up}$ spleen with the majority of B cells residing in the outer periarteriolar lymphocytic sheath area (Fig. 7 g), a distribution consistent with the activated phenotype (41, 42). IgM^{hi} IgD^{lo} marginal zone B cells were absent from $Lyn^{up/up}$ spleen and reduced in number in $Lyn^{+/up}$ spleen (Fig. 7, i and j). Increased numbers of cytoplasmic IgM^{hi} cells that are presumably plasma cells were contained within the red pulp of $Lyn^{up/up}$ spleen (Fig. 7 j). Although the absence of CD21^{hi} IgM^{hi} marginal zone B cells in $Lyn^{up/up}$ spleen (not depicted) suggests a failure in differentiation, the involvement of Lyn in the generation of this population is consistent with a previous report (43).

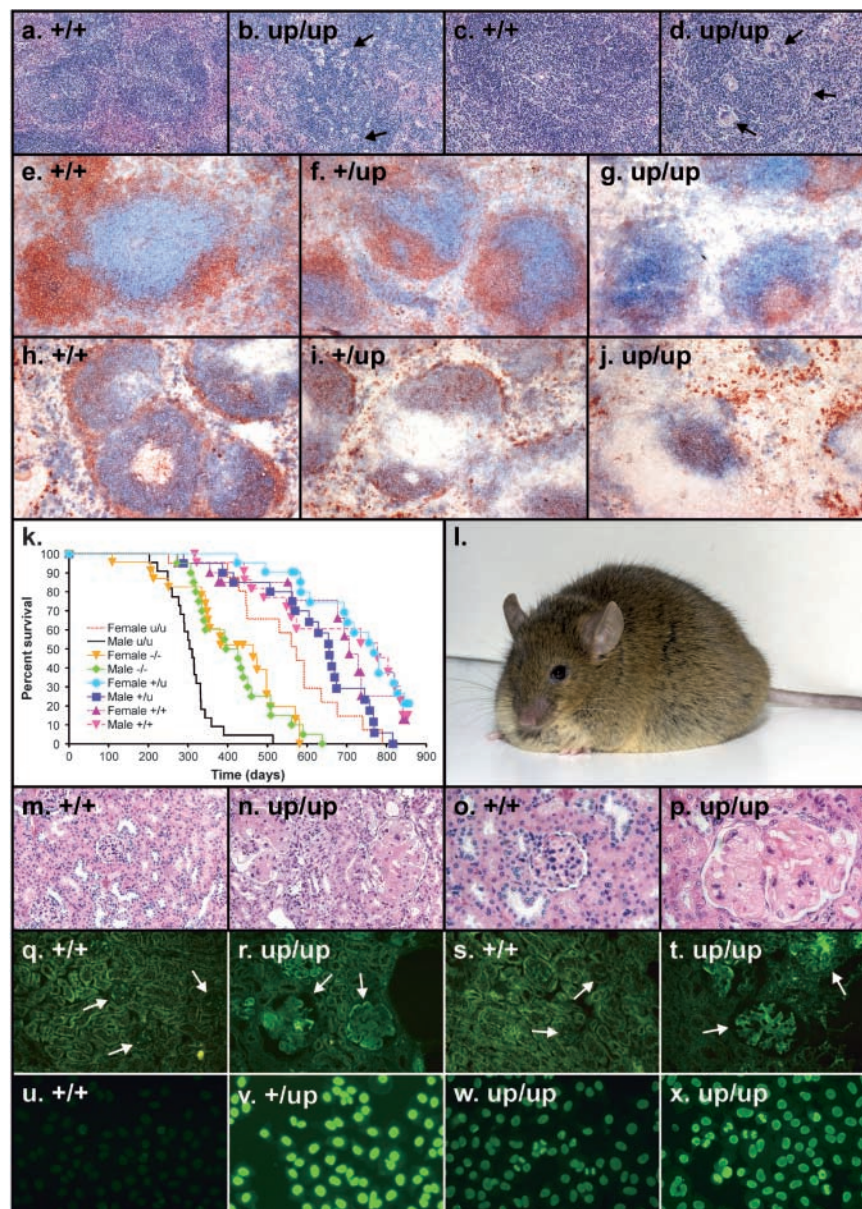


Figure 7. Histology, immunohistochemistry, survival, autoantibodies, and immunofluorescence analysis of $Lyn^{+/+}$ and Lyn mutant mice. (a) Spleen from a $Lyn^{+/+}$ mouse showing lymphoid follicles with germinal centers. (b) Spleen from a $Lyn^{up/up}$ mouse showing lymphoid follicles with numerous multinucleate giant cells (arrows). (c) Higher power view of $Lyn^{+/+}$ spleen. (d) Higher power view of $Lyn^{up/up}$ spleen depicting multinucleate giant cells within a lymphoid follicle (arrows). Spleen sections from (e) $Lyn^{+/+}$, (f) $Lyn^{+/up}$, and (g) $Lyn^{up/up}$ mice stained with B220 and CD3 to detect B (brown) and T cells (blue). Spleen sections from (h) $Lyn^{+/+}$, (i) $Lyn^{+/up}$, and (j) $Lyn^{up/up}$ mice stained with IgM (brown) and IgD (blue) to detect marginal zones (IgM^{hi}). (k) Kaplan-Meier survival curve showing the percent survival of a cohort of 20 male and 20 female $Lyn^{+/+}$, $Lyn^{+/up}$, $Lyn^{up/up}$, and $Lyn^{-/-}$ mice. (l) Male $Lyn^{up/up}$ mouse of 10 mo of age showing extensive edema. (m) Low power view of a renal cortex from a $Lyn^{+/+}$ mouse showing several normal glomeruli. (n) Low power view of $Lyn^{up/up}$ renal cortex showing two very enlarged sclerotic glomeruli. (o) High power view of $Lyn^{+/+}$ renal cortex showing a normal glomerulus. (p) High power view of $Lyn^{up/up}$ renal cortex showing a severely damaged glomerulus with lobularity and sclerosis. View of the renal cortex from (q) $Lyn^{+/+}$ and (r) $Lyn^{up/up}$ mice stained with anti-Ig. Glomeruli are indicated with arrows. View of the renal cortex from (s) $Lyn^{+/+}$ and (t) $Lyn^{up/up}$ mice stained with anti-IgG. Glomeruli are indicated with arrows. Immunofluorescence analysis of HEP-2 cells stained with antisera from (u) female $Lyn^{+/+}$, (v) male $Lyn^{+/up}$, (w) female $Lyn^{up/up}$, and (x) male $Lyn^{up/up}$ mice.

Pathology in Aged $Lyn^{up/up}$ Mice. To determine if $Lyn^{up/up}$ mice develop any pathology during the course of their lives, cohorts of control and Lyn mutant mice were aged (Fig. 7 k). In these groups the median survival of male and female $Lyn^{up/up}$ mice was 310 and 575 d, respectively (Fig. 7 k). In contrast, male and female $Lyn^{-/-}$ mice had similar survival rates of 430 and 460 d, respectively (Fig. 7 k). Male and female mice carrying a single copy of the Lyn gain-of-function mutation had median survival rates of 660 and 770 d, respectively, significantly better than $Lyn^{up/up}$ mice. However, although the median survival of female $Lyn^{+/up}$ mice was similar to the median survival of 710 d for female $Lyn^{+/+}$ mice, it is clear that male $Lyn^{+/up}$ mice have a poorer survival than male $Lyn^{+/+}$ mice (median survival of 780 d; Fig. 7 k).

From ~ 8 mo of age, a proportion of male $Lyn^{up/up}$ mice showed signs of edema (Fig. 7 l) and respiratory distress, whereas others appeared emaciated. Mice with edema had fluid collection under the skin and in pleural and peritoneal cavities, and their hearts were enlarged. Histological examination of solid organs from both edematous and emaciated $Lyn^{up/up}$ mice demonstrated severe renal disease (Fig. 7, m–p). Kidneys from these mice exhibited glomerulonephropathy, similar to membranous glomerulonephritis in humans. Glomeruli were enlarged with a relative lack of cellularity and showed thickened glomerular capillary basement membranes. In some cases, glomerulosclerosis was noted (Fig. 7, n and p). Periodic acid silver staining showed the presence of periodic acid silver–positive materials within the capillary basement membrane (not depicted). These severe kidney changes correlated with renal failure and are almost certainly the cause of the severe edema observed in the majority of older male mice. Because this form of glomerulonephritis in humans is associated with the nephrotic syndrome, characterized by severe edema, it is likely that the edema is a direct affect of the membranous-type glomerulonephritis. Although it is clear that male $Lyn^{up/up}$ mice succumb to renal failure at an earlier age than female $Lyn^{up/up}$ mice (Fig. 7 k), female $Lyn^{up/up}$ mice do show evidence of mild glomerular disease but the disease is less severe and of later onset.

The animals in the survival cohort were of a mixed C57BL/6 \times 129/Sv genetic background and because genetic background can influence development of autoimmune disease, we subsequently backcrossed the Lyn^{up} mutation for 10 generations onto the C57BL/6 background. Although only a limited number of mice have been available for analysis, $Lyn^{up/up}$ mice on the C57BL/6 background develop edema and membranous glomerulonephropathy with the same sex bias as mice on the mixed genetic background (not depicted).

$Lyn^{up/up}$ Mice Have Circulating Autoreactive Antibodies and Display Immune Complex Deposition in the Kidney. The kidney abnormalities in aged $Lyn^{up/up}$ mice are reminiscent of the lupus-like disease we and others observed in Lyn -deficient animals (24, 25). To determine whether the renal disease in aged $Lyn^{up/up}$ mice was due to an underlying autoimmune disease, we stained frozen sections of kidney with Abs to Ig (Fig. 7, q and r) and with Abs to IgG (Fig. 7,

s and t). Small patches of immune complexes could be observed in the glomeruli of $Lyn^{+/+}$ mice but these were not composed of the more pathogenic IgG Abs (Fig. 7, q and s). In kidney sections of two different $Lyn^{up/up}$ mice, strong glomerular staining was observed with Abs to Ig and IgG (Fig. 7, r and t). The presence of immune complexes in $Lyn^{up/up}$ glomeruli was confirmed by electron microscopy through the identification of subendothelial and mesangial electron dense deposits and widespread epithelial cell foot process effacement (not depicted).

The presence of serum autoantibodies was tested by staining slides of HEP-2 cells with serum from five $Lyn^{+/+}$, $Lyn^{+/up}$, and $Lyn^{up/up}$ mice of each sex. Serum from male and female $Lyn^{+/+}$ animals showed weak or no staining (Fig. 7 u and unpublished data), whereas serum from five female $Lyn^{up/up}$ mice and four out of five male $Lyn^{up/up}$ mice had antinuclear Abs (Fig. 7, w and x). Thus, although autoantibodies are clearly present in female $Lyn^{up/up}$ serum, for unknown reasons these animals develop a milder form of glomerulonephritis than their male counterparts. Antinuclear Abs were also detected in $Lyn^{+/up}$ mice, although not until ~ 2 yr of age (Fig. 7 v). These data imply that the pathology associated with $Lyn^{up/up}$ mice is a consequence of circulating autoreactive antibodies.

Discussion

To understand how the Lyn tyrosine kinase regulates signaling thresholds within B cells, we have analyzed mice carrying a gain-of-function mutation in the endogenous Lyn gene ($Lyn^{up/up}$ mice). Lyn has been implicated in both positive and negative signaling pathways in B lymphocytes (14) and, although Lyn has the capacity to both activate and inhibit BCR signaling depending on its substrates, these two functions need to be tightly regulated in order to achieve an appropriate signal transduction response. Therefore, it was of interest to determine the effect of simultaneous sustained activation by Lyn of both stimulatory and inhibitory signaling pathways. Our biochemical studies demonstrate that $Lyn^{up/up}$ B cells display constitutive phosphorylation of both positive and negative regulators of BCR signaling. However, although $Lyn^{up/up}$ B cells do not proliferate in response to B cell–derived signals, fail to develop a blast-like appearance, and induce activation markers in response to BCR cross-linking, they show exaggerated BCR–dependent calcium fluxes.

Mechanisms of B cell tolerance have been explored using model systems in which immunoglobulin transgenic B cells develop in the continuous presence of their ligand. These systems have shown that self-reactive B cells are deleted in the BM at an immature stage when the avidity of the interaction is high (44–46) but appear in the periphery in a state of arrested activation, a condition termed anergy (47, 48), when the avidity is moderate. Intriguingly, several of the phenotypic and functional characteristics of $Lyn^{up/up}$ B cells are reminiscent of the anergic B cells obtained from a model system in which mice express transgenes encoding soluble hen egg lysozyme (HEL) and a

high affinity, HEL-specific Ab (26). Such tolerant HEL-specific B cells, chronically engaged by circulating self-antigen, down-regulate surface IgM, but not IgD (49), have reduced splenic half-life (50), and although defective in BCR-mediated functions such as induction of tyrosine phosphorylation (51), can still respond to T cell-mediated signals (52). Tolerant HEL-specific B cells show elevated basal calcium oscillations but in vitro ligation with HEL fails to evoke a large, transient increase in $[Ca^{2+}]_i$ (53). $Lyn^{up/up}$ B cells show down-regulation of surface IgM (Fig. 3), defective BCR-induced responses (Fig. 5, a and b), normal responses to T cell-derived signals (Figs. 5 and 6), and reduced splenic B cell half-life (Fig. 5 c), all of which are reminiscent of anergic B cells. Spleens from both $Lyn^{up/up}$ mice and double transgenic HEL/anti-HEL mice show a striking loss of marginal zones (Fig. 7; reference 54). The abnormal distribution of B cells within splenic white pulp (Fig. 7) is also similar to the self-reactive B cells in the HEL system (42, 55). In contrast, $Lyn^{up/up}$ B cells show elevated constitutive tyrosine phosphorylation that remains inducible after BCR stimulation (Fig. 1) and heightened calcium responses after BCR ligation (Fig. 5 d). Thus, although $Lyn^{up/up}$ B cells display cellular characteristics associated with immunological unresponsiveness, their molecular profile suggests that this is achieved by actively balancing BCR-associated positive and negative regulatory pathways.

What then causes the eventual breakdown in tolerance in $Lyn^{up/up}$ mice? Although the exact cause is unknown, the following possibilities are consistent with our data. First, the diminished BCR responsiveness of $Lyn^{up/up}$ B cells may select for a higher than normal degree of self-reactivity amongst the peripheral B lymphocyte population. Such selective recruitment of self-reactivity is apparent in mice whose B cells are unresponsive to BCR ligation due to the absence of CD45 (56). Second, the molecular silencing of self-reactive B cells that usually accompanies their appearance in the periphery (51) is not enforceable in $Lyn^{up/up}$ B cells. In sharp contrast to CD45-deficient mice (56) and other models of B cell anergy (53), $Lyn^{up/up}$ B cells retain the ability to initiate and sustain both tyrosine phosphorylation and calcium flux after BCR ligation. The discordance between repertoire selection on the one hand and BCR-associated signal transduction on the other may eventually allow sufficient self-reactive cells to escape their anergic state and initiate disease.

A second pathway to autoimmunity in $Lyn^{up/up}$ mice may lie in their elevated numbers of B1 cells; a cell type that is associated with the production of natural antibodies and connected with the induction of autoimmunity (57). 8–10-fold increased numbers of B1a cells are consistently found in the peritoneal cavities of $Lyn^{up/up}$ mice and less frequently, in the circulation and other tissues. Finding more B1 cells in $Lyn^{up/up}$ spleen might be significant, given the recent report of the location-dependent responsiveness of such cells (58). $Lyn^{up/up}$ mice have slightly elevated levels of IgM, but reduced levels of most other Ig isotypes, suggesting that the IgM may well derive from the elevated B1

cell population. Perhaps not too surprisingly, $Lyn^{up/up}$ mice also have higher levels of intestinal IgM (not depicted). It will be important to determine the etiology of autoimmune disease in $Lyn^{up/up}$ mice and transplantation studies with B1 cells may define their role in the disease process. Although the nature of the autoimmune disease that $Lyn^{up/up}$ mice develop indicates that B cells play an important role in its pathogenesis, they are unlikely to act alone. T cells, which do not express Lyn, must also be recruited into the disease to give rise to the pathological IgG-mediated condition that is manifest by these mice. Therefore, it is relevant that $Lyn^{up/up}$ B cells remain receptive to T cell-derived stimuli. Other cell types such as macrophages may also contribute to the disease process.

It is interesting to compare and contrast the phenotypes of $Lyn^{up/up}$ and Lyn-deficient B cells, and as one may predict, they are almost diametrical. $Lyn^{up/up}$ B cells exhibit dramatically reduced proliferative responses to BCR stimulation, whereas Lyn-deficient B cells are hyperresponsive to anti-IgM (15, 23). Lyn-deficient B cells have relatively normal but delayed patterns of antigen-induced protein tyrosine phosphorylation (15, 23), whereas unstimulated $Lyn^{up/up}$ B cells show constitutive tyrosine phosphorylation of both positive and negative regulators of BCR signaling and have only modest increases in phosphorylation after BCR cross-linking. B1a B cells are elevated in $Lyn^{up/up}$ mice but reduced in Lyn-deficient mice (unpublished data), and serum Ig levels are reduced or relatively unchanged in $Lyn^{up/up}$ mice but elevated in Lyn-deficient mice (24, 25, 38). Notwithstanding these many differences, both strains of mice show a breakdown in self-tolerance and develop circulating autoreactive antibodies and severe lupus-like glomerulonephritis. These studies clearly demonstrate that Lyn is a key regulator of signaling in B lymphocytes and suggest that any imbalance of signaling, either by deletion or constitutive activation of Lyn, results in severe autoimmunity. Given the central role of Lyn in regulating tolerance in mouse models, its contribution to autoimmune disease in humans warrants close examination.

The authors would like to thank Steven Stacker and Antony Burgess for critically reading the manuscript. We are grateful to Paul Waring for assistance with pathology, Dianne Grail for help with animal procedures, and Roslyn Clark, Natalie Evans, Kristina Zlatic, and Amanda Light for technical assistance. We also acknowledge Val Feakes for histology preparation, Stephen Cody for assistance with photography, Janna Stickland for preparation of artwork, and Elsbeth Richardson, Teleah Rich, and Melissa Arnold for animal husbandry.

M.L. Hibbs is the recipient of a Senior Research Fellowship from the Australian Research Council, K.W. Harder is supported by a Terry Fox Post Doctoral Research Fellowship from the National Cancer Institute of Canada, and D.M. Tarlinton is a Research Fellow of the NH&MRC Australia. This work was supported in part by grants from the NH&MRC Australia and the Anti-Cancer Council Victoria.

Submitted: 2 April 2002

Revised: 1 November 2002

Accepted: 4 November 2002

References

1. Healy, J.I., and C.C. Goodnow. 1998. Positive versus negative signaling by lymphocyte antigen receptors. *Annu. Rev. Immunol.* 16:645–670.
2. O'Keefe, T.L., G.T. Williams, S.L. Davies, and M.S. Neuberger. 1996. Hyperresponsive B cells in CD22-deficient mice. *Science.* 274:798–801.
3. Sato, S., A.S. Miller, M. Inaoki, C.B. Bock, P.J. Jansen, M.L. Tang, and T.F. Tedder. 1996. CD22 is both a positive and negative regulator of B-lymphocyte antigen receptor signal transduction: altered signaling in CD22-deficient mice. *Immunity.* 5:551–562.
4. Otipoby, K.L., K.B. Andersson, K.E. Draves, S.J. Klaus, A.G. Garr, J.D. Kerner, R.M. Perlmutter, C.-L. Law, and E.A. Clark. 1996. CD22 regulates thymus independent responses and the lifespan of B cells. *Nature.* 384:634–637.
5. Nitschke, L., R. Carsetti, B. Ocker, G. Kohler, and M.C. Lamers. 1997. CD22 is a negative regulator of B cell receptor signaling. *Curr. Biol.* 7:133–143.
6. Nishimura, H., M. Nose, H. Hiai, N. Minato, and T. Honjo. 1999. Development of lupus-like autoimmune diseases by disruption of the PD-1 gene encoding an ITIM motif-carrying immunoreceptor. *Immunity.* 11:141–151.
7. Bolland, S., and J.V. Ravetch. 2000. Spontaneous autoimmune disease in Fc(gamma)RIIB-deficient mice results from strain-specific epistasis. *Immunity.* 13:277–285.
8. Inaoki, M., S. Sato, B.C. Weintraub, C.C. Goodnow, and T.F. Tedder. 1997. CD19-regulated signaling thresholds control peripheral tolerance and autoantibody production in B-lymphocytes. *J. Exp. Med.* 186:1923–1931.
9. Tamir, I., J.M. Dal Porto, and J.C. Cambier. 2000. Cytoplasmic protein tyrosine phosphatases SHP-1 and SHP-2: regulators of B cell signal transduction. *Curr. Opin. Immunol.* 12:307–315.
10. Schultz, L.D., and M.C. Green. 1976. Motheaten, an immunodeficient mutant of the mouse. II. Depressed immune competence and elevated serum immunoglobulins. *J. Immunol.* 116:936–943.
11. Shultz, L.D., P.A. Schweitzer, T.V. Rajan, T. Yi, J.N. Ihle, R.J. Matthews, M.L. Thomas, and D.R. Beier. 1993. Mutations at the murine motheaten locus are within the hematopoietic cell protein-tyrosine phosphatase (Hcph) gene. *Cell.* 73:1445–1454.
12. Tsui, H.W., K.A. Siminovitch, L. de Souza, and F.W. Tsui. 1993. Motheaten and viable motheaten mice have mutations in the hematopoietic cell phosphatase gene. *Nat. Genet.* 4:124–129.
13. Latour, S., and A. Veillette. 2001. Proximal protein tyrosine kinases in immunoreceptor signaling. *Curr. Opin. Immunol.* 13:299–306.
14. Campbell, K.S. 1999. Signal transduction from the B cell antigen receptor. *Curr. Opin. Immunol.* 11:256–264.
15. Wang, J., T. Koizumi, and T. Watanabe. 1996. Altered antigen receptor signaling and impaired Fas-mediated apoptosis of B cells in *Lyn*-deficient mice. *J. Exp. Med.* 184:831–838.
16. Smith, K.G.C., D.M. Tarlinton, G.M. Doody, M.L. Hibbs, and D.T. Fearon. 1998. Inhibition of the B cell by CD22: a requirement for *Lyn*. *J. Exp. Med.* 187:807–811.
17. Cornall, R.J., J.G. Cyster, M.L. Hibbs, A.R. Dunn, K.L. Otipoby, E.A. Clark, and C.C. Goodnow. 1998. Polygenic regulation of complex traits in autoimmunity: *lyn* kinase, CD22, and SHP-1 phosphatase are limiting elements of a biochemical pathway that regulates BCR signaling and selection. *Immunity.* 8:1–20.
18. Chan, V.W.F., C.A. Lowell, and A.L. DeFranco. 1998. Defective negative regulation of antigen receptor signaling in *lyn*-deficient B-lymphocytes. *Curr. Biol.* 8:545–553.
19. Nishizumi, H., K. Horikawa, I. Mlinaric-Rascan, and T. Yamamoto. 1998. A double-edged kinase *Lyn*: a positive and negative regulator for antigen receptor-mediated signals. *J. Exp. Med.* 187:1343–1348.
20. Maeda, A., A.M. Scharenberg, S. Tsukada, J.B. Bolen, J.-P. Kinet, and T. Kurosaki. 1999. Paired immunoglobulin-like receptor B (PIR-B) inhibits BCR-induced activation of Syk and Btk by SHP-1. *Oncogene.* 18:2291–2297.
21. Ho, L.H., T. Uehara, C.C. Chen, H. Kubagawa, and M.D. Cooper. 1999. Constitutive tyrosine phosphorylation of the inhibitory paired Ig-like receptor PIR-B. *Proc. Natl. Acad. Sci. USA.* 96:15086–15090.
22. Cornall, R.J., C.C. Goodnow, and J.G. Cyster. 1999. Regulation of B cell antigen receptor signaling by the *Lyn*/CD22/SHP1 pathway. *Curr. Top. Microbiol. Immunol.* 244:57–68.
23. Chan, V.W.F., F. Meng, P. Soriano, A.L. DeFranco, and C.A. Lowell. 1997. Characterization of the B-lymphocyte populations in *lyn* deficient mice and the role of *lyn* in signal initiation and down regulation. *Immunity.* 7:69–81.
24. Hibbs, M.L., D.M. Tarlinton, J. Armes, D. Grail, G. Hodgson, R. Maglito, S.A. Stacker, and A.R. Dunn. 1995. Multiple defects in the immune system of *lyn*-deficient mice, culminating in autoimmune disease. *Cell.* 83:301–311.
25. Nishizumi, H., I. Taniuchi, Y. Yamanashi, D. Kitamura, D. Ilic, S. Mori, T. Watanabe, and T. Yamamoto. 1995. Impaired proliferation of peripheral B cells and indication of autoimmune disease in *Lyn*-deficient mice. *Immunity.* 3:549–560.
26. Cornall, R.J., C.C. Goodnow, and J.G. Cyster. 1995. The regulation of self-reactive B cells. *Curr. Opin. Immunol.* 7:804–811.
27. Harder, K.W., L.M. Parsons, J. Armes, N. Evans, N. Kountouri, R. Clark, C. Quilici, D. Grail, G.S. Hodgson, A.R. Dunn, et al. 2001. Gain- and loss-of-function *Lyn* mutant mice define a critical inhibitory role for *Lyn* in the myeloid lineage. *Immunity.* 15:603–615.
28. Kincade, P.W., C.J. Paige, R.M. Parkhouse, and G. Lee. 1978. Characterization of murine colony-forming B cells. I. Distribution, resistance to anti-immunoglobulin antibodies, and expression of Ia antigens. *J. Immunol.* 120:1289–1294.
29. O'Reilly, L.A., A.W. Harris, D.M. Tarlinton, L.M. Corcoran, and A. Strasser. 1997. Expression of a *bcl-2* transgene reduces proliferation and slows turnover of developing B-lymphocytes in vivo. *J. Immunol.* 159:2301–2311.
30. Lalor, P.A., G.J.V. Nossal, R.D. Sanderson, and M.G. McHeyzer-Williams. 1992. Functional and molecular characterization of single, (4-hydroxy-3-nitrophenyl)acetyl (NP)-specific IgG1⁺ B cells from antibody-secreting and memory B cell pathways in the C57BL/6 immune response to NP. *Eur. J. Immunol.* 22:3001–3011.
31. Smith, K.G.C., U. Weiss, K. Rajewsky, G.J.V. Nossal, and D.M. Tarlinton. 1994. *Bcl-2* increases memory B cell recruitment but does not perturb selection in germinal centers. *Immunity.* 1:803–813.
32. van Dijk, T.B., E. van den Akker, M. Parren-van Amelsvoort, H. Mano, B. Lowenberg, and M. von Lindern. 2000.

- Stem cell factor induces phosphatidylinositol-kinase-dependent Lyn/Tec/Dok-1 complex formation in hematopoietic cells. *Blood*. 96:3406–3413.
33. Mizuno, K., Y. Tagawa, K. Mitomo, Y. Arimura, N. Hatanano, T. Katagiri, M. Ogimoto, and H. Yakura. 2000. Src homology region 2 (SH2) domain-containing phosphatase-1 dephosphorylates B cell linker protein/SH2 domain leukocyte protein of 65 kDa and selectively regulates c-Jun NH2-terminal kinase activation in B cells. *J. Immunol.* 165:1344–1351.
 34. Ono, M., S. Bolland, P. Tempst, and J.V. Ravetch. 1996. Role of the inositol phosphatase SHIP in negative regulation of the immune system by the receptor Fc(gamma)RIIB. *Nature*. 383:263–266.
 35. Liu, Q., A.J. Oliveira-Dos-Santos, S. Mariathasan, D. Boucharad, J. Jones, R. Sarao, I. Kozieradzki, P.S. Ohashi, J.M. Penninger, and D.J. Dumont. 1998. The inositol polyphosphate 5-phosphatase ship is a crucial negative regulator of B cell antigen receptor signaling. *J. Exp. Med.* 188:1333–1342.
 36. Marshall, A.J., H. Niirio, T.J. Yun, and E.A. Clark. 2000. Regulation of B-cell activation and differentiation by the phosphatidylinositol 3-kinase and phospholipase Cgamma pathway. *Immunol. Rev.* 176:30–46.
 37. Hardy, R.R., C.E. Carmack, and K. Hayakawa. 1994. Distinctive developmental origins and specificities of murine CD5⁺ B cells. *Immunol. Rev.* 137:91–118.
 38. Janas, M.L., P. Hodgkin, M.L. Hibbs, and D.M. Tarlinton. 1999. Genetic evidence for Lyn as a negative regulator of IL-4 signaling. *J. Immunol.* 163:4192–4198.
 39. Forster, I., and K. Rajewsky. 1987. Expansion and functional activity of Ly-1⁺ B cells upon transfer of peritoneal cells into allotype-congenic, newborn mice. *Eur. J. Immunol.* 17:521–528.
 40. Saginario, C., H. Sterling, C. Beckers, R. Kobayashi, M. Solimena, E. Ullu, and A. Vignery. 1998. MFR, a putative receptor mediating the fusion of macrophages. *Mol. Cell. Biol.* 18:6213–6223.
 41. Cyster, J.G., and C.C. Goodnow. 1995. Antigen-induced exclusion from follicles and anergy are separate and complementary processes that influence peripheral B cell fate. *Immunity*. 3:691–701.
 42. Fulcher, D.A., A.B. Lyons, S.L. Korn, M.C. Cook, C. Koleda, C. Parish, G.B. Fazekas de St, and A. Basten. 1996. The fate of self-reactive B cells depends primarily on the degree of antigen receptor engagement and availability of T cell help. *J. Exp. Med.* 183:2313–2328.
 43. Seo, S., J. Buckler, and J. Erikson. 2001. Novel roles for Lyn in B cell migration and lipopolysaccharide responsiveness revealed using anti-double-stranded DNA Ig transgenic mice. *J. Immunol.* 166:3710–3716.
 44. Nemazee, D.A., and K. Buerki. 1989. Clonal deletion of B-lymphocytes in a transgenic mouse bearing anti-MHC class I antibody genes. *Nature*. 337:562–566.
 45. Hartley, S.B., J. Crosbie, R. Brink, A.B. Kantor, A. Basten, and C.C. Goodnow. 1991. Elimination from peripheral lymphoid tissues of self-reactive B-lymphocytes recognizing membrane-bound antigens. *Nature*. 353:765–769.
 46. Chen, C., Z. Nagy, M.Z. Radic, R.R. Hardy, D. Huszar, S.A. Camper, and M. Weigert. 1995. The site and stage of anti-DNA B-cell deletion. *Nature*. 373:252–255.
 47. Nossal, G.J., and B.L. Pike. 1980. Clonal anergy: persistence in tolerant mice of antigen-binding B-lymphocytes incapable of responding to antigen or mitogen. *Proc. Natl. Acad. Sci. USA*. 77:1602–1606.
 48. Goodnow, C.C., J. Crosbie, S. Adelstein, T.B. Lavoie, S.J. Smith-Gill, R.A. Brink, H. Pritchard-Briscoe, J.S. Wotherpoon, R.H. Loblay, K. Raphael, et al. 1988. Altered immunoglobulin expression and functional silencing of self-reactive B-lymphocytes in transgenic mice. *Nature*. 334:676–682.
 49. Goodnow, C.C., J. Crosbie, H. Jorgensen, R.A. Brink, and A. Basten. 1989. Induction of self-tolerance in mature peripheral B-lymphocytes. *Nature*. 342:385–391.
 50. Fulcher, D.A., and A. Basten. 1994. Reduced life span of anergic self-reactive B cells in a double-transgenic model. *J. Exp. Med.* 179:125–134.
 51. Cooke, M.P., A.W. Heath, K.M. Shokat, Y. Zeng, F.D. Finkelman, P.S. Linsley, M. Howard, and C.C. Goodnow. 1994. Immunoglobulin signal transduction guides the specificity of B cell-T cell interactions and is blocked in tolerant self-reactive B cells. *J. Exp. Med.* 179:425–438.
 52. Eris, J.M., A. Basten, R. Brink, K. Doherty, M.R. Kehry, and P.D. Hodgkin. 1994. Anergic self-reactive B cells present self antigen and respond normally to CD40-dependent T-cell signals but are defective in antigen-receptor-mediated functions. *Proc. Natl. Acad. Sci. USA*. 91:4392–4396.
 53. Healy, J.I., R.E. Dolmetsch, L.A. Timmerman, J.G. Cyster, M.L. Thomas, G.R. Crabtree, R.S. Lewis, and C.C. Goodnow. 1997. Different nuclear signals are activated by the B cell receptor during positive versus negative signaling. *Immunity*. 6:419–428.
 54. Mason, D.Y., M. Jones, and C.C. Goodnow. 1992. Development and follicular localization of tolerant B-lymphocytes in lysozyme/anti-lysozyme IgM/IgD transgenic mice. *Int. Immunol.* 4:163–175.
 55. Cyster, J.G., S.B. Hartley, and C.C. Goodnow. 1994. Competition for follicular niches excludes self-reactive cells from the recirculating B-cell repertoire. *Nature*. 371:389–395.
 56. Cyster, J.G., J.I. Healy, K. Kishihara, T.W. Mak, M.L. Thomas, and C.C. Goodnow. 1996. Regulation of B-lymphocyte negative and positive selection by tyrosine phosphatase CD45. *Nature*. 381:325–328.
 57. Fagarasan, S., N. Watanabe, and T. Honjo. 2000. Generation, expansion, migration and activation of mouse B1 cells. *Immunol. Rev.* 176:205–215.
 58. Chumley, M.J., J.M. Dal Porto, and J.C. Cambier. 2002. The unique antigen receptor signaling phenotype of B-1 cells is influenced by locale but induced by antigen. *J. Immunol.* 169:1735–1743.